

**Charge disproportionation in (TMTTF)<sub>2</sub>SCN observed by <sup>13</sup>C NMR**

Shigeki Fujiyama\* and Toshikazu Nakamura

*Institute for Molecular Science, Okazaki 444-8585, Japan*

(Received 23 June 2003; revised manuscript received 14 January 2004; published 7 July 2004)

The results of the <sup>13</sup>C NMR spectra and nuclear spin-lattice relaxation rate  $1/T_1$  for the quasi-one-dimensional quarter-filled organic material (TMTTF)<sub>2</sub>SCN are presented. Below the anion ordering temperature ( $T_{AO}$ ), a new broad line appears in the NMR spectra and the intensity of the distinct line owing to the inner carbon site from the inversion center is almost halved. The remarkable difference in the temperature dependence of  $1/T_1$  below  $T_{AO}$  for the two sharp lines corresponding to outer and inner carbon sites shows the development of a local electronic state. Our simple model of a charge configuration based on the electrostatic interaction between the SCN anions and TMTTF molecules is consistent with our observation of a local gap for the spin excitation. Nevertheless, we reveal that only the electrostatic interaction is insufficient to reproduce the observed divergence of the frequency shift and the linewidth of the newly appearing broad line stemming from the charge-accepting inner site at a much lower temperature than  $T_{AO}$ .

DOI: 10.1103/PhysRevB.70.045102

PACS number(s): 71.30.+h, 71.45.Lr, 75.30.Fv, 76.60.-k

**I. INTRODUCTION**

There has been considerable interest in quasi-one-dimensional (Q1D) correlated electrons. Theoretical studies on generalized Hubbard model for Q1D electronic systems have revealed a rich phase diagram including various instabilities towards spin-Peierls, antiferromagnets, spin density wave (SDW) and the superconductivity.<sup>1,2</sup>

The physical properties of the molecular-based Q1D quarter-filled materials (TMTCF)<sub>2</sub>X [ $C=Se(S)$ ], also known as the Bechgaard salts (and their sulphur analogs), have been extensively studied so far because the materials realize various ground states by modifying calcogens ( $C$ ) and anions ( $X$ ).<sup>3</sup> The macroscopic electronic properties of (TMTCF)<sub>2</sub>X are summarized in a pressure ( $P$ ) versus temperature ( $T$ ) phase diagram.<sup>4</sup>

The resistivities of the (TMTTF)<sub>2</sub>X ( $C=S$ ) are two orders higher than those of (TMTSF)<sub>2</sub>X ( $C=Se$ ). The temperatures where the resistivities show their minima are about 200 K, which is one order higher than those for TMTSF materials.<sup>5,6</sup> In addition, the ground states of the TMTTF family are driven by magnetic instabilities undergoing spin-Peierls or antiferromagnetic phase transitions, although those of TMTSF are driven by Fermi surface instabilities towards incommensurate SDW or superconductivity. This implies that strong electronic correlation becomes relevant for the electronic states of the TMTTF materials at low  $T$ .

Recently, it is argued that the electronic charges are disproportionated along the chain direction by measuring the dielectric response,<sup>7</sup> x-ray diffraction (XRD),<sup>8,9</sup> and <sup>13</sup>C NMR spectra, and relaxation rate in the semiconducting  $T$  region.<sup>10,11</sup> Theoretical studies on quarter-filled-Q1D electronic systems based on extended Hubbard models assuming on-site and intersite repulsions predict several electronic instabilities toward  $2k_F$  SDW,  $2k_F$  charge density waves (CDW), and  $4k_F$  CDW including their coexistences.<sup>12-17</sup>

The ground state of (TMTTF)<sub>2</sub>SCN is revealed to be the commensurate antiferromagnet from the antiferromagnetic resonance.<sup>18</sup> The dependence of the <sup>1</sup>H-NMR spectra on the

direction of the external magnetic field suggests that nodes of spin density exist on the TMTTF molecules.<sup>19,20</sup> Reference 12 proposed a periodic (up-0-down-0) magnetic structure for antiferromagnetic state in this material for analysis of the NMR spectra. They also pointed out that the intersite repulsive interaction is indispensable to reproduce the charge disproportionated ground state in mean-field calculations, which concludes the  $4k_F$  CDW state at low  $T$ .

In this paper, we demonstrate the charge disproportionation in (TMTTF)<sub>2</sub>SCN by the <sup>13</sup>C NMR spectra, which is triggered by anion ordering. The contrasting  $T$  dependence of the linewidth of the spectra and nuclear spin lattice relaxation rates  $1/T_1$  for distinct lines indicates that anion ordering generates local and random electronics states at the inner carbon site. The results of  $1/T_1$  also suggests that charge disproportionation occurs only at the inner carbon site, since  $1/T_1$  for the outer carbon remains almost intact at  $T_{AO}$ . We argue a charge configuration below  $T_{AO}$  by comparing the results of XRD. The model assuming that the dominating source to disproportionate the electronic charges is the electrostatic interaction between the anions and the molecules leads to the  $4k_F$  CDW charge configuration. Moreover, the results of XRD indicate that the random displacements of anions from the original position or the anion ordering with finite correlation length even below  $T_{AO}$  reproduce the local and random electronic states at finite temperatures.

However, the divergence of the frequency shift and the linewidth of the broad line stemming from the charge-accepting inner site at a temperature much lower than  $T_{AO}$  needs other sources to generate the slowing down of the charge fluctuations than the electrostatic interaction. We discuss the possible frustration between the disordered electronic state owing to the imperfect anion ordering and the CDW instability due to the global  $\pi$ electron correlation for the Q1D quarter-filled electronic systems.

**II. EXPERIMENTS**

A rectangular-plate-like single crystal of (TMTTF)<sub>2</sub>SCN in which the two central carbon sites on the TMTTF mol-

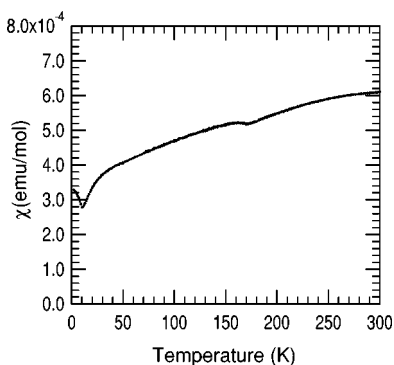


FIG. 1. The  $T$  dependence of the uniform susceptibility measured by a superconducting quantum interference device SQUID at an external field of 5.0 T.

ecules are labeled with  $^{13}\text{C}$  was prepared by the standard electrochemical oxidation method. The uniform susceptibility of our sample is shown in Fig. 1. As shown in Fig. 1, the uniform susceptibility ( $\chi$ ) in the paramagnetic state gradually decreases in lowering temperature with a small dip at  $T_{\text{AO}} \sim 170$  K. Below 40 K, the  $\chi$  shows a stronger decrease than that above 40 K.

The NMR measurements were performed by using a standard pulsed NMR spectrometer operated at 87.12 MHz with the bandwidth of 300 kHz for the single crystal. The spectra were obtained by the Fourier transformation (FT) of the solid echo refocused by applying a pair of  $\pi/2$  pulses shifted in phase by  $\pi/2$ . The nuclear recovery data were obtained by the integration of the distinct lines in the frequency domain by the saturation recovery method. The  $1/T_1$  were obtained by fitting them to a single-exponential formula.

### III. $^{13}\text{C}$ NMR SPECTRA

We show in Fig. 2 the  $^{13}\text{C}$  NMR spectra of  $(\text{TMTTF})_2\text{SCN}$  in the paramagnetic state. We applied the external magnetic field along the *magic angle* to overlap the doubly split absorption lines due to the nuclear dipolar inter-

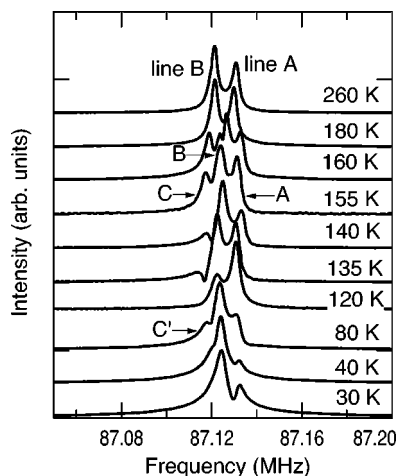


FIG. 2.  $^{13}\text{C}$  NMR spectra of  $(\text{TMTTF})_2\text{SCN}$  in the paramagnetic state.

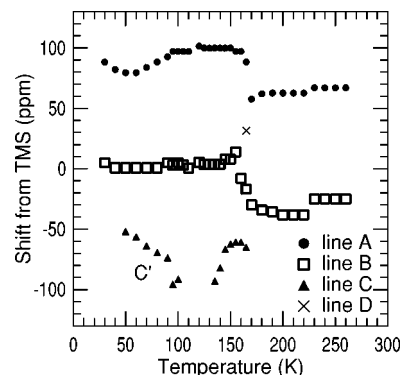


FIG. 3. Frequency shifts from TMS in the paramagnetic state.

action. The observed two distinct lines at room temperature correspond to two inequivalent carbon sites: one is the outer carbon site from the inversion center in the unit cell, and the other is the inner site. The molecular orbital calculation predicts that the spin density on the inner carbon site is almost 1.4 times as large as that on the outer site in the TMTTF molecules.<sup>3,21</sup> We also plot in Fig. 3 the frequency shifts from TMS (tetramethylsilane) of the distinct lines of the spectra as a function of  $T$ .

According to the molecular orbital calculation, the dominating character of the central carbon site participating in the highest occupied molecular orbital is the  $2p_z$  orbital, where  $z$  is the direction perpendicular to the plane of the TMTTF molecule. If the dipolar field from other orbitals than  $^{13}\text{C}$   $2p_z$  is neglected, the frequency shift  $K$  is expected to have the uniaxial symmetry,  $K(\theta) = K_{\text{iso}} + (3 \cos^2 \theta - 1)K_{\text{ax}}$ . Here  $\theta$  is the angle between the external field and the  $z$  axis,  $K_{\text{iso}}$  ( $K_{\text{ax}}$ ) is the isotropic (anisotropic) part of the magnetic frequency shift, which is related to the spin susceptibility ( $\chi$ ) by  $K_{\text{iso,ax}} = F_{\text{iso,ax}} \chi / 2N_A \mu_B$ . Here,  $N_A$  is Avogadro's number and  $\mu_B$  is the Bohr magneton. The quantity  $F_{\text{ax}}$  is proportional to the spin density in the  $2p_z$  orbital as  $F_{\text{ax}} = \frac{2}{5} \langle r^{-3} \rangle_{2p} \mu_B \sigma$  (Refs. 22 and 23). Here  $\langle r^{-3} \rangle_{2p}$  is the expectation value of  $r^{-3}$  for the  $2p_z$  orbital of the central carbon site and  $\sigma$  is the fractional spin density in the orbital. In our experimental condition, the  $z$  axis is almost perpendicular to the external field; therefore, the spin density  $\sigma$  in the  $2p_z$  orbital of the  $^{13}\text{C}$  is expected to reduce the total hyperfine coupling constant, which results in the small  $T$  dependence of  $K$  above 180 K as shown in Fig. 3.

In lowering the temperature, two lines split into four lines between 165 K and 160 K. However, only three lines are observed below 160 K as shown in Figs. 2 and 3.

It is well known that noncentrosymmetric anions in  $(\text{TMTCF})_2\text{X}$  can take two orientations in the crystal. At room temperature, the directions of the anions are disordered, which results in the fact that the inversion centers are present on average only. Below the anion ordering temperature ( $T_{\text{AO}}$ ), a superstructure is observed by XRD measurements, which reveals that the wave vector of the anion ordering in  $(\text{TMTTF})_2\text{SCN}$  is  $\mathbf{q} = (0, 1/2, 1/2)$  (Ref. 24). This exhibits that the superstructure is not in the chain ( $a$ ) direction.

The variation of the NMR spectra can be easily ascribed to the structural phase transition at  $T_{\text{AO}}$ . Four lines are ob-

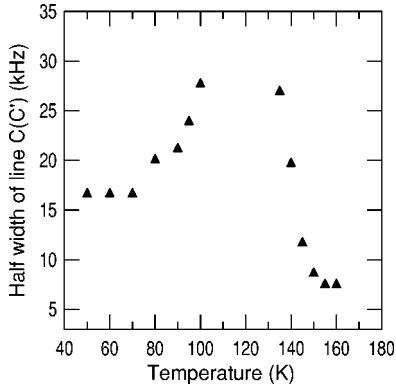


FIG. 4. The frequency difference between the peak position and the 20% point of the maximum value for the line  $C(C')$  on the low-frequency side.

served in the spectra in the narrow  $T$  range of a transitional state between the anion disordered and ordered states. Between 135 K and 155 K, the NMR spectra are decomposed into two sharp lines (lines  $A$  and  $B$  henceforth) and one broadened line (line  $C$ ). It should be noted that the intensity of line  $A$ , which is located at the highest frequency in the spectrum, is almost halved below  $T_{AO}$ . The frequency shifts of lines  $A$  and  $B$  show little  $T$  dependence between 50 K and 155 K, which indicates that the spin densities at the carbon sites corresponding to both lines are unchanged or less than those above  $T_{AO}$ . In contrast, line  $C$  progressively shifts to the smaller-frequency side with line broadening in lowering the temperature. At 130 K, line  $C$  disappears and only lines  $A$  and  $B$  remain in the spectra. However, a new broad line ( $C'$ ) becomes visible below 100 K. As shown in Fig. 3, line  $C'$  shifts in the opposite manner to line  $C$  with the turning point around 120 K and finally merges into line  $B$  at 50 K. We also plot the half width at the 20% maximum of line  $C(C')$  in Fig. 4. As shown in Fig. 4, the linewidth becomes broader in decreasing temperature between 160 K and 135 K, which indicates a wide distribution of the charge density or the slowing down of the local spin fluctuation for line  $C$ . Approaching 135 K, the width of line  $C$  diverges and finally line  $C$  disappears. Below 100 K where line  $C'$  appears, the linewidth becomes smaller in lowering the temperature. Since the uniform susceptibility is almost constant between 50 and 170 K, the origin of the large shift and the divergence of the width of line  $C$  has to be attributed to the local variation of the electronic state at the carbon site.

#### IV. NUCLEAR SPIN-LATTICE RELAXATION RATE

We show in Fig. 5 the nuclear spin-lattice relaxation rate of  $^{13}\text{C}$ ,  $1/T_1$ , for the distinct lines.  $1/T_1$  for the line  $A$  ( $1/T_1^A$ ) and that for the line  $B$  ( $1/T_1^B$ ) increase with temperature in a parallel manner above  $T_{AO}$  in the logarithmic scale as shown in Fig. 5. The  $1/T_1$  at site  $n$  is expressed as,  $1/T_1^n = (2\gamma_n^2 T / \mu_B^2) \sum_q {}^n F_{\perp}(q)^2 \chi''(q, \omega_L) / \omega_L$ ; here,  $\gamma_n$  is the gyromagnetic ratio of carbon,  ${}^n F_{\perp}(q)$  is the  $q$ -dependent hyperfine coupling constant at site  $n$ ,  $\chi''$  is the imaginary part of

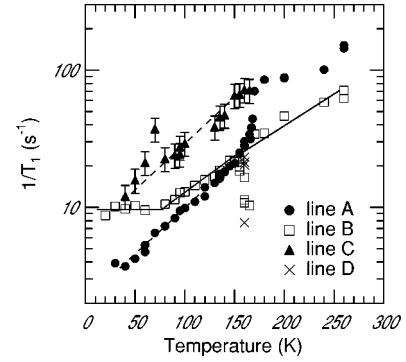


FIG. 5. Nuclear spin-lattice relaxation rates for distinct lines. The solid and dashed lines are guides to the eye.

the dynamic susceptibility, and  $\omega_L$  is the Larmor frequency. Thus, the only difference between  $1/T_1^A$  and  $1/T_1^B$  comes from that of  ${}^n F_{\perp}(q)$ . Since the local spin correlation function is expected to have little  $q$  dependence in organic conductors, which results in uniform hyperfine coupling constants, the  $F_{\perp}(q)$  exclusively depends on the spin density at the nucleus. Since  $1/T_1^A$  appears twice as large as  $1/T_1^B$  above  $T_{AO}$ , we conclude that line  $A$  in the frequency domain is due to the inner carbon site in the TMTTF molecule.

In the narrow  $T$  range between 160 and 170 K where four distinct lines are observed in the NMR spectra,  $1/T_1^B$  (solid square) shows a marked decrease. The  $1/T_1^B$  at 165 K becomes almost half of  $1/T_1^B$  at 170 K, but is recovered at 160 K. The small dip within a 10 K interval is also observed in the uniform susceptibility as shown in Fig. 1. Below 160 K,  $1/T_1^B$  again decreases in lowering the temperature down to 60 K and has a crossover to the low- $T$  regime where  $1/T_1^B$  becomes independent of  $T$ . This crossover is discussed experimentally and theoretically in Refs. 25 and 26 in the framework of weakly interacting Q1D electronic systems.

On the other hand,  $1/T_1^A$  (solid circle) changes differently from  $1/T_1^B$  for  $T$  below  $T_{AO}$ .  $1/T_1^A$  strongly decreases from 170 K to 140 K compared with that in the metallic state. Since  $1/T_1^B$  shows much a more moderate  $T$  dependence in this  $T$  range, the only source of the marked decrease of  $1/T_1^A$  is the loss of hyperfine coupling  $|{}^A F_{\perp}(q)|$  and the corresponding loss of charge density at site  $A$ .

Below 140 K, the  $1/T_1^A$  continues to decrease more steeply than  $1/T_1^B$  in lowering the temperature. The  $1/T_1^A$  is almost same with  $1/T_1^B$  at 140 K but becomes less than half with  $1/T_1^B$  at 40 K. Therefore, the nuclear relaxation process below  $T_{AO}$  for line  $A$  is concluded to be insensitive to the uniform susceptibility ( $\chi$ ) and seems to have a gap for the local spin excitation spectra. We plot  $1/T_1^A$  as a function of  $1/T$  in the logarithmic scale in Fig. 6. The observation of the convex curve in Fig. 6 indicates that the activation energy  $\Delta$  decreases in lowering the temperature. The solid (dashed) straight line corresponds to  $\Delta = 200$  K (70 K) in the activated  $T$  dependence of  $1/T_1 \propto \exp(-\Delta/T)$ . It should be mentioned that  $\Delta$  is comparable to the temperature, indicating that the nuclear relaxation process at site  $A$  originates from the electronic correlation of thermally excited two magnons beyond the random barriers.

We also plot  $1/T_1$  for lines  $C$  and  $C'$  in Fig. 5 by solid triangles. The  $1/T_1^C$  is three times as large as  $1/T_1^A$  at 150 K

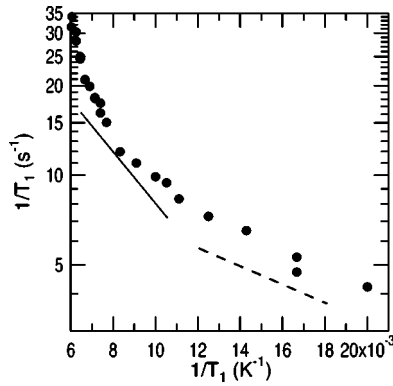


FIG. 6. Arrhenius plot of the nuclear spin-lattice relaxation rate for line A below 150 K. The solid (dashed) line shows the activated  $T$  dependence with  $\Delta=200$  K (70 K) by a crude fitting of the data between 140 K and 100 K (between 100 K and 40 K) to the formula  $1/T_1 \propto \exp(-\Delta/T)$ .

and decreases in lowering the temperature in an almost parallel manner with  $1/T_1^A$ . It is noticeable that  $1/T_1^{C'}$  follows the extrapolated line of  $1/T_1^C$  between 150 K and 130 K, which indicates similar spin densities for both lines. Therefore we consider that line  $C'$  is assigned to the same carbon site as line  $C$ .

## V. DISCUSSION

The prominent features of the frequency shifts and  $1/T_1$  for distinct lines of the  $^{13}\text{C}$  NMR in Secs. III and IV can be summarized as follows. A broad line appears below  $T_{\text{AO}}$ , which can be ascribed to the charge disproportionation probably triggered by the anion ordering. Second is the remarkable difference in the  $T$  dependences of  $1/T_1$ 's for the lines A(C) and B, which indicates an unexpected local fluctuation of electronic charges and the random potential for lines A and C below  $T_{\text{AO}}$ . And the third is the disappearance of line C( $C'$ ) at a temperature well below  $T_{\text{AO}}$ .

We discuss the charge disproportionation shown by the NMR spectra and the local electronic state indicated by  $1/T_1$ 's for lines A and B by comparing the results of XRD (Ref. 24) in Sec. V A. We propose a possible charge configuration that is naturally led by the superstructure of the ordered anions assuming that the dominating source for the charge disproportionation is the electrostatic interaction. This discussion discriminates the electronic correlation from the trivial electrostatic interactions stemming from the anion ordering.

In Sec. V B, we discuss the divergence of the frequency shift and the linewidth of line C, which cannot be understood in the framework of Sec. V A.

### A. Charge disproportionation triggered by anion ordering

Our observation of the three distinct lines in the NMR spectra below  $T_{\text{AO}}$  shows that the electronic charges are disproportionated probably triggered by the anion ordering. The results of  $1/T_1^B$  that follows the uniform susceptibility and the remarkable decrease of  $1/T_1^A$  just below  $T_{\text{AO}}$  between

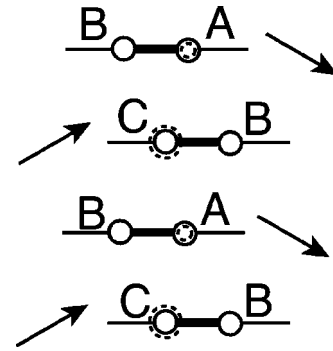


FIG. 7. Schematic representation of the anion configuration that realizes  $q=(0,1/2,1/2)$ .<sup>24</sup> The arrows symbolize the short contact interaction to one inner carbon site in TMTTF molecules. The circles represent two carbon sites in the TMTTF molecules, and the symbols A, C (inner carbons) and B (outer carbon) correspond to the distinct lines in the NMR spectra discussed in the text.

170 K and 145 K which is one-third of  $1/T_1^C$  indicate the variation of the local electronic state in the molecules.

The results of XRD show the loss of inversion symmetry in the unit cell below  $T_{\text{AO}}$ , and the configuration of SCN anions are proposed to be schematically represented by the arrows in Fig. 7.<sup>24</sup> They argued that the anions alternately establish long and short contacts along the  $a$  (chain) direction. If we assume that the dominating source to shift the charge densities at the carbon sites is the electrostatic interaction between the ordered anions and the molecules, much more effect on the charge density at the inner carbon site than that at the outer carbon is expected.

Since the  $1/T_1^B$  remains almost intact at  $T_{\text{AO}}$ , the charge disproportionation can be considered to take place exclusively at the inner sites. That results in the possible charge configuration as shown Fig. 7. As shown in Fig. 7, the superstructure of the anion ordering leads to the charge disproportionation alternation with period 2. This charge configuration can realize the local electronic state that is observed in  $1/T_1^A$  below  $T_{\text{AO}}$ .

### B. Wipeout of line C and the electronic correlation between the molecules

As mentioned in Sec. IV, lines C and  $C'$  are assigned to the same carbon site because of the same magnitudes of the spin densities for both lines. We discuss here the disappearance of line C( $C'$ ) between 130 K and 100 K.

The loss of the NMR intensity observed for line C is known as a “wipeout” phenomenon when the electronic state is inhomogeneous, causing a broadening of the NMR spectra and a shortening of the spin-echo decay time.<sup>27,28</sup> In low-dimensional correlated electronic materials, it is reported that the intensity of the Cu NQR spectrum in the two-dimensional  $\text{CuO}_2$  plane of  $\text{La}_{2-x}\text{Ba}(\text{Sr})_x\text{CuO}_4$  decreases in lowering the temperature, in which microscopic charge ordering is argued.<sup>29</sup> For the Q1D cuprates, the intensity of the Cu NMR spectra of the hole-doped  $\text{Cu}_2\text{O}_3$  two-leg ladder,  $\text{Sr}_{14-x}\text{Ca}_x\text{Cu}_{24}\text{O}_{41}$ , decreases in the semiconducting  $T$  regime in lowering the temperature.<sup>30</sup> In these cases, the shortening

of the spin-echo decay time ( $T_2$ ) due to the strong spin fluctuation in the vicinity of charge stripes or the slow fluctuation of the electric field gradients generates the wipeout of the NMR spectra. In the present study, the most plausible origin of the wipeout is also the shortening of the spin-echo decay time due to the slowing down of charge fluctuations because the frequency shift and the linewidth of the NMR spectra diverge at around 120 K. Since it is known that  $1/T_2$  takes a maximum value when the inverse of the correlation time of electronic fluctuations is close to the second moment of the NMR spectrum, the fluctuation frequency of the local field is confirmed to be less than 50 kHz below 120 K.<sup>31</sup>

It is noteworthy that the critical phenomenon observed for site C occurs at a much lower temperature than  $T_{AO}$ . In addition, no significant anomaly in the macroscopic measurements such as resistivity and uniform susceptibility has been reported around 120 K so far, and  $1/T_1^B$ , which follows the uniform susceptibility, remains intact around this temperature. Therefore the significant slowing down of electronic charges may be due to local electronic interactions.

It is reported that the superspot at  $q=(0, 1/2, 1/2)$  in the reciprocal space appears at 160 K, and the intensity at the superspot continues to increase almost linearly down to 50 K according to XRD.<sup>32</sup> Between 160 K and 50 K where the wide distribution remains in the displacements of anions from the original position or the partial ordering with a finite correlation length, the electrostatic interaction between the anions and TMTTF molecules would lead to disordered charge densities at site C. Indeed, the observation of the activated  $T$  dependence with multibarriers in  $1/T_1^A$  reveals random potentials at site A. Since the energy scale of XRD is much higher than the Larmor frequency ( $\sim 100$  MHz), our observation of the divergence of the linewidth for line C(C') observed at an intermediate temperature between the onset and the saturating temperature for the anion ordering shows that it cannot be concluded that the only source of the strong slowing down of the local charge fluctuation at site C is the electrostatic coupling between the anions and molecules. Instead, it is plausible that some source that can compete with the disordered electronic state generates a frustration at the carbon site below  $T_{AO}$ .

It is recently argued that some members of the (TMTTF)<sub>2</sub>X family have a charge disproportionated phase of  $4k_F$  CDW in the semiconducting  $T$  regime. It is reported that the distinct two lines of <sup>13</sup>C NMR spectra split at a much higher than the spin-Peierls transition temperature for (TMTTF)<sub>2</sub>MF<sub>6</sub> ( $M=As, P$ ) which has the spin-Peierls ground state.<sup>10</sup> Concerning the charge density, the ratio of  $1/T_1$ 's for the inner and outer carbon sites is independent of  $T$  even in the charge-disproportionated state. Therefore, the ratio of the charge densities between the inner and outer carbon sites is unchanged as schematically shown in Fig. 8. This charge ordering phenomenon is regarded as a result of the strong Coulomb repulsive interaction between the electrons.

Since the correlation length of this Coulomb-repulsion-driven  $4k_F$  CDW diverges below the charge disproportionation temperature, this CDW instability can compete with the disordered electronic state at the inner carbon sites generated

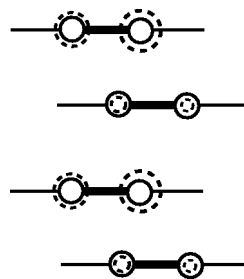


FIG. 8. Schematic view of the charge density with  $4k_F$  CDW charge disproportionation that can be realized by the strong Coulomb repulsive interaction.

by the imperfect anion ordering between 160 K and 50 K. This frustration between the global electronic correlation and the local electrostatic interaction can lead to a local gap for the spin excitations. We should mention, however, that there still remains an open question on the mechanism of the competition between these local electrostatic interaction and the global electronic correlation among the molecules. In particular, the process of the charge transfer from the microscopic viewpoint is still unresolved. We can easily quote two possibilities. One is the charge transfer simply from site A to C that can be realized only by the local interaction such as the electrostatic interaction as discussed in Sec. V A. The other is the Coulomb-repulsion-driven  $4k_F$  CDW with local charge transfer within the molecule. At the present stage, we can not pin down the detailed mechanism of charge disproportionation in this material, in which the competition between the local interaction and the global electronic correlation is crucial to realize our results of NMR spectra and nuclear relaxations. Theoretical studies that include the interactions between the anions and molecules are expected.

## VI. CONCLUSION

We measured the <sup>13</sup>C NMR spectra and nuclear spin lattice relaxation rate  $1/T_1$  for (TMTTF)<sub>2</sub>SCN, which has a linear anion. The appearance of the new broad line (line C) below the anion ordering temperature ( $T_{AO}$ ) reveals that the electronic charges are disproportionated in this material.

In contrast to (TMTTF)<sub>2</sub>MF<sub>6</sub> that have spin-Peierls ground states, the charge transfer in this material leads to the local fluctuations of electronic charges which induces the different  $T$  dependences in the frequency shifts and  $1/T_1$ . Of these, the strong decrease of  $1/T_1$  just below  $T_{AO}$  for the charge donating site (site A) in lowering the temperature revealed an activation gap for spin excitations and the inhomogeneous electronic state possibly due to the wide distribution of the displacements from the original position of the anions as observed by XRD.

These results are consistent with the wave vector of anion ordering which naturally leads to  $4k_F$ -CDW-like charge disproportionation by assuming the electrostatic interaction between the anions and molecules.

However, the divergence of the frequency shift and the linewidth of the broad line stemming from the charge-accepting inner site at a temperature much lower than  $T_{AO}$

needs other sources to generate the slowing down of the charge fluctuations than the electrostatic interaction. We propose the  $4k_F$  CDW instability due to the global  $\pi$  electron correlation as a candidate that can make a frustrated electronic state between the disordered electronic state.

#### ACKNOWLEDGMENTS

One of the authors (S.F.) is grateful to Professor Yonemitsu for a critical reading of the manuscript. We are also

grateful to Professor Yakushi, Professor Brazovskii, Professor Hosokoshi, Dr. Hiraki, and Dr. Yamamoto for fruitful discussions. This work is supported by a Grant-in-Aid for Scientific Research on Priority Area, "Development of Molecular Conductors and Magnets of New Functionality by Spin-Control" from the Ministry of Education, Culture, Sports, Science and Technology, and by a Grant-in-Aid for Scientific Research (No. 13640375) from Japan Society for the Promotion of Science.

\*Present address: Department of Applied Physics, University of Tokyo, Hongo, Bunkyo-ku, Tokyo 113-8656, Japan. Electronic address: fujiyama@ap.t.u-tokyo.ac.jp

<sup>1</sup>H. J. Schultz, in *Strongly Correlated Electronic Materials*, edited by K. S. Bedell, Z. Wang, D. E. Meltzer, A. V. Balatsky, and E. Abrahams (Addison-Wesley, Reading, MA, 1994).

<sup>2</sup>J.-I. Kishine and K. Yonemitsu, *Int. J. Mod. Phys. B* **16**, 711 (2002).

<sup>3</sup>As a review, see *Organic Superconductors*, 2nd ed., edited by T. Ishiguro, K. Yamaji, and G. Saito (Springer-Verlag, Heidelberg, 1998).

<sup>4</sup>D. Jérôme, *Science* **252**, 1509 (1991).

<sup>5</sup>P. Delhaes, C. Coulon, J. Amiel, S. Flandrois, E. Toreilles, J. M. Fabre, and L. Giral, *Mol. Cryst. Liq. Cryst.* **50**, 43 (1979).

<sup>6</sup>R. Laversanne, C. Coulon, B. Gallois, J. P. Pouget, and R. Moret, *J. Phys. (France) Lett.* **45**, L393 (1984).

<sup>7</sup>F. Nad, P. Monceau, and J. M. Fabre, *Eur. Phys. J. B* **3**, 301 (1998); F. Nad, P. Monceau, C. Carcel, and J. M. Fabre, *Phys. Rev. B* **62**, 1753 (2000).

<sup>8</sup>J. P. Pouget and S. Ravy, *Synth. Met.* **85**, 1523 (1997).

<sup>9</sup>Y. Nogami and T. Nakamura, *J. Phys. IV* **12**, Pr9-145 (2002).

<sup>10</sup>D. S. Chow, F. Zamborszky, B. Alavi, D. J. Tantillo, A. Baur, C. A. Merlic, and S. E. Brown, *Phys. Rev. Lett.* **85**, 1698 (2000).

<sup>11</sup>F. Zamborszky, W. Yu, W. Raas, S. E. Brown, B. Alavi, C. A. Merlic, and A. Baur, *Phys. Rev. B* **66**, 081103 (2002).

<sup>12</sup>H. Seo and H. Fukuyama, *J. Phys. Soc. Jpn.* **66**, 1249 (1997).

<sup>13</sup>N. Kobayashi and M. Ogata, *J. Phys. Soc. Jpn.* **66**, 3356 (1997); N. Kobayashi, M. Ogata, and K. Yonemitsu, *ibid.* **67**, 1098 (1998).

<sup>14</sup>K. C. Ung, S. Mazumdar, and D. Toussaint, *Phys. Rev. Lett.* **73**, 2603 (1994).

<sup>15</sup>S. Mazumdar, S. Ramasesha, R. T. Clay, and D. K. Campbell,

*Phys. Rev. Lett.* **82**, 1522 (1999).

<sup>16</sup>S. Mazumdar, R. T. Clay, and D. K. Campbell, *Phys. Rev. B* **62**, 13400 (2000).

<sup>17</sup>R. T. Clay, S. Mazumdar, and D. K. Campbell, *Phys. Rev. B* **67**, 115121 (2003).

<sup>18</sup>C. Coulon, A. Maaroufi, J. Amiel, E. Dupart, S. Flandrois, P. Delhaes, R. Moret, J. P. Pouget, and J. P. Morand, *Phys. Rev. B* **26**, 6322 (1982).

<sup>19</sup>T. Nakamura, R. Kinami, T. Takahashi, and G. Saito, *Synth. Met.* **86**, 2053 (1997).

<sup>20</sup>T. Nakamura, T. Nobutoki, Y. Kobayashi, T. Takahashi, and G. Saito, *Synth. Met.* **70**, 1293 (1995).

<sup>21</sup>N. Kinoshita, M. Tokumoto, H. Anzai, T. Ishiguro, G. Saito, T. Yamabe, and H. Teramae, *J. Phys. Soc. Jpn.* **53**, 1504 (1984).

<sup>22</sup>A. Abragam and M. H. Pryce, *Proc. R. Soc. London, Ser. A* **205**, 135 (1961).

<sup>23</sup>J. Owen and J. H. M. Thornley, *Rep. Prog. Phys.* **29**, 675 (1966).

<sup>24</sup>J. P. Pouget and S. Ravy, *J. Phys. I* **6**, 1501 (1996).

<sup>25</sup>P. Wzietek, F. Creuzet, C. Bourbonnais, D. Jérôme, K. Bechgaard, and P. Batail, *J. Phys. I* **3**, 171 (1993).

<sup>26</sup>C. Bourbonnais, *J. Phys. I* **3**, 143 (1993).

<sup>27</sup>A. Abragam, *The Principles of Nuclear Magnetism* (Oxford University Press, Oxford, 1961).

<sup>28</sup>J. Winter, *Magnetic Resonance in Metals* (Oxford University Press, Oxford, 1971).

<sup>29</sup>A. W. Hunt, P. M. Singer, K. R. Thurber, and T. Imai, *Phys. Rev. Lett.* **82**, 4300 (1999).

<sup>30</sup>S. Fujiyama, M. Takigawa, S. Horii, N. Motoyama, H. Eisaki, and S. Uchida, *J. Phys. Chem. Solids* **63**, 1119 (2002); S. Fujiyama, Ph.D. thesis. University of Tokyo, 2001.

<sup>31</sup>M. Takigawa and G. Saito, *J. Phys. Soc. Jpn.* **55**, 1233 (1986).

<sup>32</sup>J. P. Pouget, *J. Phys. IV* **10**, 43 (2000).